# Accepted Manuscript

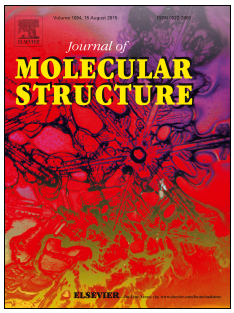


Novel benzildihydrazone based Schiff bases: Syntheses, characterization, thermal properties, theoretical DFT calculations and biological activity studies

Gökhan Elmacı, Halil Duyar, Burcu Aydıner, Issah Yahaya, Nurgül Seferoğlu, Ertan Şahin, Süheyla Pınar Çelik, Leyla Açık, Zeynel Seferoğlu

PII: S0022-2860(19)30122-X

DOI: https://doi.org/10.1016/j.molstruc.2019.01.104

Reference: MOLSTR 26155

To appear in: *Journal of Molecular Structure*

Received Date: 31 August 2018

Revised Date: 12 December 2018

Accepted Date: 30 January 2019

Please cite this article as: Gö. Elmacı, H. Duyar, B. Aydıner, I. Yahaya, Nurgü. Seferoğlu, E. Şahin, Sü.Pı. Çelik, L. Açık, Z. Seferoğlu, Novel benzildihydrazone based Schiff bases: Syntheses, characterization, thermal properties, theoretical DFT calculations and biological activity studies, *Journal of Molecular Structure* (2019), doi: https://doi.org/10.1016/j.molstruc.2019.01.104.

Graphical Abstract

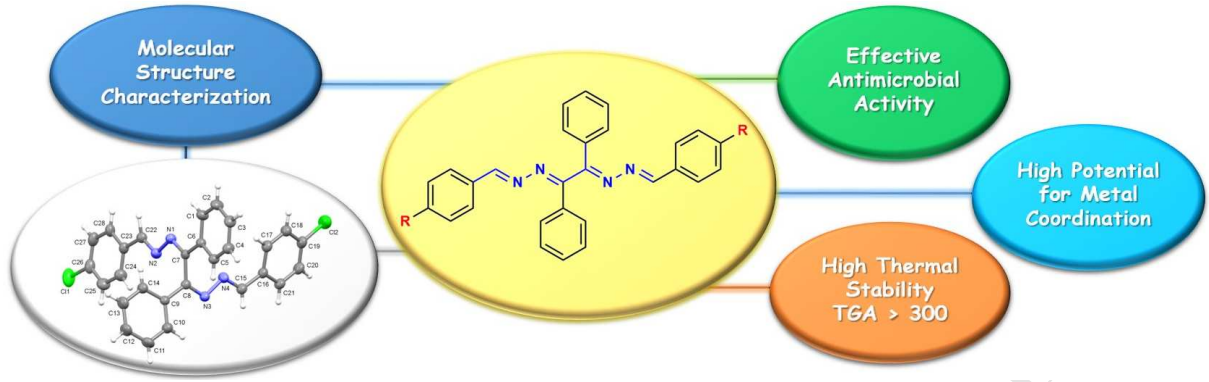

# Novel benzildihydrazone based Schiff bases: Syntheses, characterization, thermal properties, theoretical DFT calculations and biological activity studies

Gökhan Elmacı[a], Halil Duyar[b], Burcu Aydıner[b], Issah Yahaya[b], Nurgül Seferoğlu[c], Ertan Şahin[d], Süheyla Pınar Çelik[e], Leyla Açık[e], Zeynel Seferoğlu[b,*]

[a]*Department of Chemistry, Faculty of Science, Adıyaman University, Adıyaman 02040, Turkey*

[b]*Department of Chemistry, Faculty of Science, Gazi University, Teknikokullar, Ankara 06500, Turkey*

[c]*Department of Advanced Technology, Gazi University, Teknikokullar, Ankara 06500, Turkey*

[d]*Department of Chemistry, Faculty of Science, Atatürk University, Erzurum 25240, Turkey*

[e]*Department of Biology, Faculty of Science, Gazi University, Teknikokullar, Ankara 06500, Turkey*

**Corresponding author's Tel.: +90 312 2021525; fax: +90 312 2122279*

**E-mail addresses: znseferoglu@gazi.edu.tr (Z. Seferoğlu).*

**Abstract**

A novel series of benzildihydrazone derived Schiff base compounds having electron-accepting and donor-donating appendices were synthesized. A combined experimental and theoretical analysis was conducted to elucidate all the characteristic and structural features of the synthesized molecules. The experimental characterizations were performed by using FT-IR, $^{1}H/^{13}C$ NMR, mass spectroscopic techniques, and X-ray diffraction methods. The thermal stabilities of the molecules were evaluated by thermal gravimetric analysis (TGA) and all them were found to be stable above 300 $^{o}C$. To support the experimental, structural, and spectroscopic data of the dyes, the quantum chemical parameters were obtained within the density functional theory (DFT) calculations. In addition, some properties based on the HOMO and LUMO energies and the temperature dependence of some thermodynamic quantities (i.e. entropy, heat capacity, and enthalpy) were also studied. According to the antimicrobial activity evaluation results, compound **1f** has been found to be potentially effective in suppressing microbial growth of bacteria with variable potency. The DNA cleavage activity of the compounds was analyzed by gel electrophoresis assay. The results showed that the compounds have DNA cleaving activity.

*Keywords:* Benzil dihydrazone, X-ray, TGA, DFT/TD-DFT, Antimicrobial activity, DNA binding.

## 1. Introduction

In 1864, Hugo Schiff described the preparation of a Schiff base by a condensation reaction between an aldehyde and an amine [1]. Schiff bases, due to the presence of the imine group, are employed in the elucidation of the mechanism of transformation of racemization reaction in biological systems [2–5]. Different biological activities including antitumor, antibacterial, antifungal, herbicidal, etc., are studied as a result of the presence of the azomethine linkage (>C=N-) in living systems [6]. Again, Schiff base derivatives are valuable therapeutic drugs due to their potent antibacterial, antifungal, and antiviral properties [7-9]. Furthermore, Schiff bases and their analogues are frequently used as model compounds for understanding the structure-activity relationship between biomolecules and drug molecules [10-13]. Sriram *et al*. [14] reported that, antiviral prodrugs modified with Schiff bases, are highly effective against mouse hepatitis viruses (MHV) at very low concentrations ($EC_{50}$ of 1.6 μM). Mahmoud and co-researchers reported that, Cu (II) Schiff base complex, prepared by condensing 2,6-diaminopyridine with *o*-benzoyl benzoic acid, had an effect on human breast cancer cell, according to *in vitro* cytotoxicity studies they carried out [15].

Hydrazones and their metal analogues usually have biological activity and can display enzymatic reactions in cells [16-18]. Edward and co-workers have successfully reported that, the replacement of an aromatic moiety by different groups in some antibiotics may lead to the improvement of their antibiotic activity [19,20]. Beside their biological importance, due to the presence of the toxicologically vital moiety (N–C=O), hydrazones can act as potential donors for varieties of metal ions. These hydrazine based ligands contain an amide bond and have the ability to undergo a keto-enol tautomerism. Thus, they can coordinate to central metal ions via nitrogen and/or oxygen [21]. Additionally, their capability to coordinate may depend on the

pH of the medium, the nature of the substituents, and the metal they are coordinating with [22].

Understanding the effects of substituent on the properties of compounds has been a vital goal in chemistry. Libin Zang and Shimei Jiang [23] have shown how substituens have played significant roles in the sensing and selectivity of Schiff bases, appended with different substituents, towards some completing anions. Recently, I. Yahaya *et al*. [24] investigated and successfully reported the effects of changing substituents on the solubility and the absorption properties of some Schiff bases they had prepared.

Antimicrobial susceptibility testing can be used for novel drug candidate discovery, and epidemiology. Antibiotics used to treat bacterial infections are in danger of losing their efficacy because of the increase in microbial resistance [25]. The multi-drug resistant bacteria have become a global concern to public health. Therefore, there has been a growing concern in developing new antimicrobial agents to combat microbial resistance. Schiff base complexes have been used as drugs and have valuable antibacterial [26], antifungal [27], and antitumor [28] activities. In recent times, DNA has been intensively studied as the target molecule in the development of potential antiviral and anti-cancer drugs [29-31]. Non-covalent interactions between prepared candidate molecules and DNA are crucial for drug design studies [32,33]. Schiff base compounds based on benzyl dihydrazone have become well-known ligands in the design and synthesis of compounds in coordination and supramolecular chemistry, due to the simplicity in their synthesis and their coordination versatility [34,35].

In recent times, and among various applications, DNA has been intensively studied as the target molecule in the development of potential antiviral and anti-cancer drugs [36,37]. Non-covalent interactions between prepared candidate molecules and DNA are crucial for drug design studies [38,39].

In our previous studies, we synthesized, characterized, and evaluated the molecular structures of benzilmonohydrazone derived Schiff bases bearing different electro-donating and electro-accepting substituents [40,41].

Considering all the literature facts mentioned so far, we therefore realized that the synthesis of novel Schiff bases, especially those appended with benzildihydrazones, is of great importance for drug development studies and cannot over-emphasized. Therefore, in the present study, we have prepared a new series of benzildihydrazone derived Schiff bases also having different electron-accepting and electron-donating groups and conducted spectroscopic characterization. In our contribution, we focus our attention on the differences between the mono- and the dihydrazones in terms of biological and other important properties. The thermal properties of the prepared dihydrazone compounds were determined. The experimental results obtained in this study were further explained by theoretical calculations. Finally, in the investigation of the biological properties of the compounds, we focused on the interaction of the compounds with plasmid-DNA and their antimicrobial properties against some bacteria and fungi.

## 2. Experimental

### *2.1. Materials and instrumentations*

The chemicals used in the syntheses of all the compounds were obtained from Aldrich Chemical Company (USA) and were used without further purification. All reactions were magnetically stirred and monitored by thin layer chromatography (TLC), using Merck silica gel (60 F254) plates (0.25 mm) and visualized under Ultraviolet light (UV). FT-IR (ATR) spectra were recorded on Perkin-Elmer Spectrum 100 FT-IR spectrophotometer. NMR spectra

were recorded on a Bruker Avance 300 Ultra-Shield in DMSO-$d_6$. Chemical shifts are expressed in δ units (ppm). Thermal analysis of the prepared compounds was performed using Hitachi 7300 thermal analysis system at a heating rate of 20 °C $min^{-1}$ under a nitrogen flow (100 mL $min^{-1}$). Mass spectra was performed using a Waters LCT Premier XE (TOF MS) (Gazi University Laboratories, Department of Pharmacological Sciences) mass spectrometer. X-ray single crystal structure was determined on Rigaku R-axis Rapid-S IP area detector diffractometer in the Department of Chemistry, Atatürk University, Erzurum, Turkey.

*2.2. Synthesis and characterization of the compounds **1a-h***

The benzildihydrazone was prepared based on literature procedures [29,30,40,41] and used as the starting material. The Schiff base compounds **1a-h** were synthesized by mixing benzildihydrazone (0.001 mol) and corresponding aldehydes **a-h** (0.002 mol) in 20 mL dry methanol. Two drops of hydrochloric acid were added to the mixture. The mixture was then refluxed for 5 h to form the products **1a-h** (**Scheme 1**). The products obtained were then cooled and the solvent was removed by slow evaporation. All the compounds **1a-h** were recrystallized using ethyl acetate. The characterization data for all the compounds can be seen in **Figs. S1-S32** in the Supplementary Information.

**Scheme 1 is here**

*(1E,2E)-1,2-bis(((E)-benzylidene)hydrazono)-1,2-diphenylethane (**1a**)*

Yield: 70%, m.p. 110 °C. FT-IR (ATR, $\upsilon_{max.}$, $cm^{-1}$): 2979, 2937 (aromatic and aliphatic C-H stretch); 1610 (C=N stretch). $^1$H NMR (300 MHz): δ 8.57 (s, 2H); 7.80 (m, 4H); 7.62-7.30 (m,

16H). $^{13}$C NMR (75 MHz) δ: 164.8; 159.8; 134.2; 130.9; 130.7; 128.7; 128.6; 127.7. HRMS (m/z) $(M-H)^+$ calculated for $C_{28}H_{23}N_4$: 415.1923; found: 415.1923.

*(1E,2E)-1,2-bis(((E)-4-nitrobenzylidene)hydrazono)-1,2-diphenylethane (**1b**)*

Yield: 73%, m.p. 180 °C. FT-IR (ATR, $\upsilon_{max.,}$ $cm^{-1}$): 3078, 2979 (aromatic and aliphatic C-H stretch); 1615 (C=N stretch); 1317 (N-O asymmetric stretch). $^1$H NMR (300 MHz): δ 8.72 (s, 1H); 8.38 (d, *J*: 7.8 Hz, 2H); 7.82 (m, 4H); 7.53 (m, 3H). $^{13}$C NMR (75 MHz) δ: 164.8; 15.0; 149.2; 139.8; 133.4; 132.0; 129.6; 127.8; 124.5. HRMS (m/z) $(M-H)^+$ calculated for $C_{28}H_{21}N_6O_4$: 505.1624; found: 505.1621.

*4,4'-((1E,1'E)-(((1E,2E)-1,2-diphenylethane-1,2-diylidene)bis(hydrazine-2,1-diylidene))bis(methanylylidene))dibenzoic acid* (**1c**)

Yield: 68%, m.p. 345 °C. FT-IR (ATR, $\upsilon_{max.,}$ $cm^{-1}$): 3050,2970 (aromatic and aliphatic C-H stretch); 3250 – 2400 (carboxylic acid O-H stretch); 1687 (C=O stretch); 1612 (C=N stretch). $^1$H NMR (300 MHz): δ 13.14 (s, 2H); 8.64 (s, 2H); 7.92 (d, *J*: 7.2 Hz, 4H); 7.78 (m, 4H); 7.68 (d, *J*: 8.2 Hz, 4H); 7.49 (m, 6H). $^{13}$C NMR (75 MHz) δ: 167.1; 164.5; 159.9; 137.8; 133.7; 133.3; 131.8; 130.1; 129.5; 128.7; 127.7. HRMS (m/z) $(M-H)^+$ calculated for $C_{30}H_{23}N_4O_4$: 503.1719; found: 505.1621.

*(1E,2E)-1,2-bis(((E)-4-chlorobenzylidene)hydrazono)-1,2-diphenylethane (**1d**)*

Yield: 76%, m.p. 170 °C. FT-IR (ATR, $\upsilon_{max.,}$ $cm^{-1}$): 3059, 2979 (aromatic and aliphatic C-H stretch); 1609 (C=N stretch). $^1$H NMR (300 MHz): δ 8.58 (s, 2H); 7.77 (m, 4H); 7.59 (d, *J*: 8.2 Hz, 4H); 7.48 (m, 10H).$^{13}$C NMR (75 MHz) δ: 164.6; 159.7; 136.4; 133.8; 132.9; 131.7; 120.2; 129.5; 129.4; 127.7. HRMS (m/z) $(M-H)^+$ calculated for $C_{28}H_{20}Cl_2N_4$: 483.1103 ; found: 483.1113.

*(1E,2E)-1,2-bis(((E)-4-methylbenzylidene)hydrazono)-1,2-diphenylethane (**1e**)*

Yield: 74%, m.p. 125 °C. FT-IR (ATR, $\upsilon_{max.,}$ $cm^{-1}$): 3061, 2933 (aromatic and aliphatic C-H stretch); 1601 (C=N stretch). $^1$H NMR (300 MHz): δ 8.52 (s, 2H); 7.77 (m, 4H); 7.47 (m,

10H); 7.20 (d, *J*: 8.0 Hz, 4H); 2.29 (s, 6H). $^{13}$C NMR (75 MHz) δ: 164.2; 160.6; 141.9; 134.1; 131.4; 131.4; 129.8; 129.4; 128.7; 127.6; 21.5. HRMS (m/z) $(M-H)^+$ calculated for $C_{30}H_{26}N_4$: 443.2236; found: 443.2223.

*4,4'-((1E,1'E)-(((1E,2E)-1,2-diphenylethane-1,2-diylidene)bis(hydrazine-2,1-diylidene))bis(methanylylidene))diphenol (**1f**)*

Yield: 65%, m.p. 236-238 °C. FT-IR (ATR, $\upsilon_{max.,}$ $cm^{-1}$): 3300–3000 (O-H stretch); 3062, 2970 (aromatic and aliphatic C-H stretch); 1602 (C=N stretch). $^1$H NMR (300 MHz): δ 10.07 (s, 1H); 8.47 (s, 1H); 7.75 (m, 2H); 7.45 (m, 8H); 7.40 (d, *J*: 8.6 Hz, 2H); 6.76 (d, *J*: 8.6 Hz, 2H). $^{13}$C NMR (75 MHz) δ: 169.9; 161.0; 160.8; 134.4; 131.1; 130.7; 129.3; 127.5; 125.2; 116.1. HRMS (m/z) $(M-H)^+$ calculated for $C_{28}H_{23}N_4O_2$: 447.1821; found: 447.1808.

*(1E,2E)-1,2-bis(((E)-4-methoxybenzylidene)hydrazono)-1,2-diphenylethane (**1g**)*

Yield: 74%, m.p. 125 °C. FT-IR (ATR, $\upsilon_{max.,}$ $cm^{-1}$): 3061, 2933 (aromatic and aliphatic C-H stretch); 1601 (C=N stretch); 1250 (Ar-O-C). $^1$H NMR (300 MHz): δ 8.52 (s, 1H); 7,77 (m, 12H); 7.53 (d, *J*: 8.8 Hz, 2H); 7,46 (m, 12H); 6.95 (d, *J*: 8.7 Hz, 2H); 3.76 (s, 3H). $^{13}$C NMR (75 MHz) δ: 165.8; 162.2; 160.5; 134.8; 131.7; 129.3; 127.1; 125.7; 114.4; 55.3. HRMS (m/z) $(M-H)^+$ calculated for $C_{30}H_{27}N_4O_2$: 475.2123; found: 475.2124.

*4,4'-((1E,1'E)-(((1E,2E)-1,2-diphenylethane-1,2-diylidene)bis(hydrazine-2,1-diylidene))bis(methanylylidene))bis(N,N-dimethylaniline) (**1h**)*

Yield: 78%, m.p. 210 °C. FT-IR (ATR, $\upsilon_{max.,}$ $cm^{-1}$): 3060, 2918 (aromatic and aliphatic C-H stretch); 1602 (C=N stretch); 1342 – 1296 (C-N). $^1$H NMR (300 MHz): δ 8.41 (s, 1H); 7.39 (m, 2H); 7.80-7.35 (m, 5H); 6.66 (d, *J*: 8.0 Hz, 2H); 2.96 (s, 6H). $^{13}$C NMR (75 MHz) δ: 163.4; 161.1; 152.7; 130.7; 130.3; 129.2; 127.4; 121.4; 111.9; 95.6; 40.0. HRMS (m/z) $(M-H)^+$ calculated for $C_{32}H_{33}N_6$: 501.2767; found: 501.2776.

*2.3. X-ray crystallography*

For the crystal structure analysis, suitable quality of single crystals were selected. When it was necessary, the crystals were cut to obtain the appropriate size. Crystals, mounted on a Rigaku R-AXIS RAPID-S diffractometer (with $MoK_\alpha$ radiation $\lambda$=0.71069 Å) was used for the data collection. Data collections were carried out at room temperature [273 (2) K]. Integration of the intensities, correction for Lorentz and polarization effects, and cell refinement were performed using CrystalClear (Rigaku/MSC Inc.,2005) software [42]. The atomic coordinates were located using direct methods employed by SHELXS [43]. The successive refinements, once the atoms were placed in their postulated positions, were made using SHELXL [43] All non-hydrogen atoms were then refined anisotropically. The hydrogen atoms were placed in idealized positions in a riding model, after location on a Fourier difference map. An isotropic refinement was used for all hydrogen atoms and temperature factors of 1.2 or 1.5 times that of the parent atoms were assigned. The experimental data such as the crystal data, structure refinement details, etc. can be seen in **Table 1**.

**Table 1 is here**

*2.4. Computational procedures*

The calculations were performed in the framework of density functional theory (DFT) in the Gaussian 09 program package [45]. The geometric structures on the ground state were obtained using B3LYP/6-31+g(d,p) methods. The confirmation of the convergence to minima on the potential energy surface was made from the vibrational analysis for each molecule. The

electronic spectra of the compounds were also obtained from TD-DFT calculations at the same level, in DMSO and chloroform, in which the integral equation formalism of the polarizable continium model (PCM) [42,43] was employed to evaluate the solvent effects.

*2.5. Antimicrobial Activity*

The antimicrobial potency of the synthesized compounds was done by agar well diffusion technique against fungi and gram negative and positive bacteria. Compounds **1a, 1b, 1c, 1d, 1e, 1f, 1g** and **1h** were tested for their inhibitory activities against Candida albicans ATCC 10231, Candida tropicalis NRRL Y-12968, Candida krusei ATCC 6258 fungi and Bacillus subtilis ATCC 6633, Bacillus cereus NRRLB-3711, Staphylococcus aureus ATCC 25923, Enterococcus faecalis ATCC 29212, Enterococus hirae ATCC 9790, Escherichia coli ATCC 35218, Escherichia coli ATCC 25922, Pseudomonas aeruginosa ATCC 27853, Proteus vulgaris RSKK 96029, Salmonella typhimurium ATCC 14028, Klebsiella pneumaniae ATCC 13883 bacteria. The microorganisms were acquired from the collections of Gazi University Molecular Biology Culture Collection, Turkey. Ampicillin (10 µg), chloramphenicol (30 µg) (antibacterial), and ketoconazole (50 µg) (antifungal) were used for comparison as positive control. The agar plate surface was inoculated by spreading a volume of the tested strain inoculum with microbial suspension adjusted to 0.5 McFarland scale, over the agar surface. Then, a hole with a diameter of 6 to 8 mm was punched, aseptically with a sterile tip, and a volume (100 µL) of the compound at 4000 µM was introduced into the well. After that, the agar plates were incubated at 37 $^{o}$C for bacteria and 30 $^{o}$C for fungi. The antimicrobial agent diffused in the agar medium and inhibited the growth of the microbial strain tested. The diameter of the zone of growth inhibition was measured by antibiogram zone measuring scale. Each bacterial strain was sub-cultured overnight at 37 °C in LB agar. The bacteria were

processed using different concentrations of the compounds. Compound-free control tubes were included in each run. All test were replicated in three time.

*2.6. DNA binding Studies*

The stock solutions of the compounds were disolved in DMSO. Then, the aliquots of the compounds, ranging from 2000 to 250 µM, were incubated with plazmid DNA in dark at 37 $^{o}$C for 24 h. The compounds\DNA mixtures were loaded onto the agarose gel. The agarose gel electrophoresis run under TAE buffer (0.05 M Tris base, 0.05 M glacial acetic acid and 1 mM EDTA, pH=8.0) for 3 h at 70 V. After that, the gel was stained with ethidium bromide, visualized under UV light using a transilluminator (BioDoc Analyzer, Biometra) and the image was photographed with a video camera. Each test was conducted for triplicate and the mean values were taken.

*2.7. DNA Binding with the compounds*

The binding experiment of each of the compounds (**1a, 1b, 1c, 1d, 1e, 1f, 1g** and **1h**) with DNA was carried out by agarose gel electrophoresis. The plasmid-DNA and different concentrations of the compounds was incubated for 24 hours. Agarose gel electrophoresis was carried out at 70 V for 3 h in TAE buffer. DNA bands were visualized by using Biometra Transilluminator.

*2.8. Restriction enzyme digestion*

*Bam*H1 and *Hind*III are restriction endonuclease that recognize sequences 5'-G/GATCC-3', 5'-A/AGCTT and hydrolyze hosphodiester bond between adjacent guanine and adenine sites respectively. The plasmid DNA used in this study contains a single restriction site for both enzymes and these enzymes convert the supercoiled Form I and singly nicked circular Form II to linear form III DNA. Therefore conformational changes can be observed by treating DNA-compound mixture with the restriction enzymes. Each of the compound-DNA mixtures was first incubated for 24 h at 37°C and then subjected to enzyme digestion. The mixtures were left at 37°C for another 1 h and loaded onto the gel. The gel was then photographed.

## 3. Results and discussion

*3.1. X-ray diffraction analysis*

The suitable crystals of the derivatives **1d, 1e**, and **1h** were obtatained by using ethanol or methanol or a mixture of ethanol/methanol solution via slow evaporation process. After the process, suitable crystals that formed analysed using single crystal X-rays diffraction analysis. The single-crystal structures formed are shown in **Figs. 1** and **2**. Selected metrical parameters from the X-ray diffraction are listed in **Table S1** (**Supplementary Information**). The average bond lengths and bond angle parameters of the ring systems (phenyl), C=N-N=C and $-N-CH_3$ units were noted to be in the normal ranges.

**Figs. 1 and 2 are here**

The crystallographic data (**Table S2, Supplementary Information**) demonstrate that, two dihydrazon Schiff bases (**1d**,**1e**) crystallized in triclinic system with space group *P-1* and the other (**1h)** crystallized in monoclinic system with space group *P21/c*. Dibenzilidene hydrazine units were found to be nearly planar. The N-N (*hydrazine*) distances are in a typical single bond range [1.407(3)-1.430(3) Å]. The C=N double bond units in *hydrazine* have been determined to be around 1.264(3)-1.286(3) Å. The torsion angles involving the C=N-N=C units have values in the range of 137.3-180.0°. These torsion angles in all the crystals and optimized gas phase geometry were found to be in close agreement with the expected value due to the $sp^2$ hybridization of the N atoms. The C-Cl bond lengths are 1.728(3) and 1.729(3)Å. All the results realized herein are similar to those found in our previous studies [29,30,40,41]. The conformations have been defined by steric effects which forced a rotation of the *N*,*N*'-Dibenzylidene-hydrazine units relative to C7-C8 single bond axis, and these bonds vary between 1.498(3)-1.508(3)Å. One of the *N*,*N*'-dibenzilidene-hydrazine groups of each molecule was more planar, the other units were significantly twisted around their molecular axis. For these turn around units, the dihedral angles formed by LSQ-planes of C16/C21 and C9/C14 phenyl rings have been determined to be 28.11(2)° (for **1d**), 23.24(4)° (for **1e**), and 61.48( 2)° (for **1h**).

The *Cl*1⋯*Cl*1 intermolecular interactions were considered as the primary reason for the layered structure of the dichloride (**1d**) crystal. The distance *d*(Cl•••Cl) = 3.383(4) Å (3) was found to be sufficiently less than the sum of the vdW radii (3.52 Å). The π-π stacking interactions between the delocalized π-electrons of the phenyl rings have been found to be relatively weak. The distance between the rings centroids were obtained in the range of 3.9–4.3 Å. The crystal packings are also controlled by non-classical weak C-Cl⋯*Cg* and C-H⋯*Cg* (pi-ring) interactions (**Table S3, Supplementary Information**).

*3.2. Computational analysis*

*3.2.1. Optimized structures*

The optimized geometries of all the studied molecules (**1a**-**1h**) are illustrated in **Fig. 3**. The selected optimized structural parameters are given in **Table 1** and compared with the experimental data of **1d, 1e**, and **1h**. The calculated parameters are in good agreement with X-ray results for **1d**, **1e** and **1h**. The correlation coefficient ($R^2$) obtained from the comparison of X-ray and computed bond lengths are found as $R^2$= 0.98 for **1d**, $R^2$=0.96 for **1e** and $R^2$=0.97 for **1h**. Comparison of the parameters of the other molecules, without X-ray data, with **1d**, **1e** and **1h** showed that they have similar geometry with **1d**, **1e** and **1h**. The Ph-C=N-N=C-Ph moieties have been found to be in the anti-form and a significant conjugation was noticed as a result of the planarity of the C16, C15, N4, N3, C8, and C9 atoms in one moiety, and the C6, C7, N1, N2, C22, and C23 atoms, in the other moiety, as seen from the dihedral angles (**Table S1, Supplementary Information**). In addition, two *Ph*-C=N-N=C-Ph moieties are almost perpendicular to each other with the dihedral angle N3-C8-C7-N1 changes in the range 94.5-96.1$^o$.

**Fig. 3 is here**

*3.2.2. Absorption spectra of **1a**-**1h***

The absorption spectra were obtained in DMSO (ε = 46.45 Debye) and chloroform (ε = 4.81 Debye) both experimentally and theoretically. The absorption spectra of compounds **1a-h** were recorded over the λ range of 300-700 nm using a variety of solvents with concentration

range of $10^{-6}$-$10^{-8}$ M (**Table 1**). Using calculations, the absorption spectra were also obtained by employing the TD-DFT methods with 6-31+G(d,p) basis set. The experimental and theoretical results are shown in **Table 1**. According to the experimental spectra results, all the molecules have strong absorption band in the range 322-397 nm in DMSO, and 309-380 nm in chloroform, and are attributed to π-π* transitions. The comparison of the absorption maxima ($\lambda_{max}$) of **1b**, **1c** and **1d**, with that of **1a** indicated that, the largest bathochromic shift (19 nm) has been observed for **1b** which is appended with a strong electron withdrawing (-$NO_2$) group, and there was no significant changes for **1c** and **1d**, which were appended with -COOH and –Cl, at the para position on the phenyl rings, respectively. Similarly, the electron-donating groups at the para position of the phenyl rings affected the absorption spectra. There was a shift in the range 7-19 nm, relative to **1a**, for receptors **1g**, **1f**, and **1e**, having electron-donating groups –$CH_3$, -OH, -$OCH_3$, respectively. The biggest shift (75 nm) was realized for **1h** which the strongest electron-donating group, –$N(CH_3)_2$, among the derivatives that have electron-donating substituents. Similar behaviors were observed for the absorption spectra recorded in chloroform. On the other hand, the effects of the solvents on the absorption spectra for each molecule could also be appreciated as shown in **Fig. 1** and **Table 1**. The smallest bathochromic shifts occurred in the absorption spectra of **1c** and **1g** while the largest bathochromic shifts were seen for the other molecules due to the increasing dielectric constant from chloroform to DMSO. The calculated maximum wavelength values are in agreement with the experimental values, whereas the solvent effects and substituent effects were not observed in the calculation results. The biggest deviation of experimental values was obtained as 84 nm for **1b** in chloroform, and the smallest as 10 nm for **1e** in DMSO. It could be noted that, the reason for these discrepancies between the experimental and the theoretical results is that, the geometries were obtained in the gas phase whereas the experimental parameters refer to the crystalline form of the molecules.

**Table 1 is here**

*3.2.3. HOMO-LUMO gaps and global reactivities of **1a-1h***

The highest occupied molecular orbital and the lowest unoccupied molecular orbital energies (i.e. $E_{HOMO}$ and $E_{LUMO}$) and the energy gap (ΔE) between the HOMO and the LUMO can be used to determine the molecular properties of the molecules, such as stability and reactivity. While the instability and the ability of the electron donating are characterized with high $E_{HOMO}$ value, the ability of the electron accepting is related to the lower $E_{LUMO}$ value. However, small ΔE value refers to a molecule having more polarizable, high chemical reactivity, and low kinetic stability [48].

The diagram of the HOMO and LUMO of the studied molecules are shown in Fig.S33 and the $E_{HOMO}$ and $E_{LUMO}$ values obtained from the optimized geometries and ΔE values of the molecules are presented in **Table S4** (**Supplementary Information**). The ionization energy (I), electron affinity (A), electronic chemical potential (μ), global hardness (η), global electrophilicity index (ω), softness (s), and the expressions used to determine them from $E_{HOMO}$ and $E_{LUMO}$ are also given in **Table S4**. Derivative **1h** has higher capability of donating electrons than the rest because it is having the highest $E_{HOMO}$ and the lowest electrophilicity index (ω). Similarly, **1b** has lower $E_{LUMO}$, the highest ω values, and its electron accepting ability is higher. The largest energy gap has been estimated to be 3.96 eV for **1a**, indicating that **1a** should be a harder molecule with good stability, it is also having the highest chemical hardness ($\eta$=1.98 eV) among the studied molecules.

*3.2.4. Thermodynamic properties*

The thermodynamic functions were obtained from the vibrational analysis with 6-31+g(d,p) basis set in gas phase. The temperature variations of the heat capacity at constant pressure ($C_p$), entropy (S), and enthalpy (H), with respect to the zero-temperature (T=0 K) for **1d**, **1e** and **1h**, are demonstrated in **Fig. 4**. As illustrated in **Fig. 4**, the $C_p$, S, and the ΔH increase from 200 K to 1000 K, which is caused by the rise of molecular vibrations with increasing temperature.

**Fig. 4 is here**

*3.2.5. Thermal Analysis*

The TGA curve for the prepared Schiff bases is depicted in **Fig. 5**. As shown in TGA curve, the decomposition process starts at about 300 °C and proceeds rapidly with increasing temperature until about 330 °C (**Table S5**). The order of thermal stability of samples is: (**1g**)~ (**1h**) > (**1e**) ~ (**1d**) ~ (**1a**) > (**1b**) ~ (**1c**) ~ (**1f**). No direct connection has been observed between the thermal stability and the effect(s) substituent(s). Molecules (**1f**) and (**1h**) can exhibit intermolecular hydrogen bonding between the compounds and the substituent groups. The relatively high melting points of (**1f**) and (**1h**) may be related to the strong intermolecular H-bonding in the crystal structures of the molecules.

**Fig. 5 is here**

*3.2.6. Antimicrobial activity*

All the Schiff base compounds **1a-h** were used to evaluate their antibacterial activity against bacteria and yeast species. Evaluation of antibacterial activity of the compounds was recorded and is shown in **Table 2**. The results show that, only compound **1f** is potentially effective in suppressing microbial growth of bacteria with variable potency. Compound **1f** also showed activity towards *Bacillus subtilis* ATCC 6633 (G+), *Staphylococcus aureus* ATCC 25923 (G+), *Enterococcus faecalis* ATCC 29212 (G+). In addition, all the compounds did not show any antifungal activity against the tested yeast strain.

**Table 2 is here**

*3.2.7. DNA-compound binding*

The results show conformational changes due to compounds-DNA interactions as well as compounds binding sites and sequence preference. The DNA cleavage was determined by the relaxation of supercoiled circular Form I of plasmid DNA into the linear Form III. If supercoiled circular plasmid DNA is subjected to agarose gel electrophoresis, the fastest migration will be observed for supercoiled Form I DNA. If one strand is cleaved, the supercoils will relax to produce a slower moving open circular Form II DNA. If both strands are cleaved, a linear Form III DNA is generated which migrates in between Form I and Form II [49].

When plasmid DNA was interacted with decreasing concentrations of the compound mixture (**compounds 1a**, **1b**, **1c, 1d, 1e, 1f, 1g** and **1h)**, two DNA bands corresponding to Forms II and III were observed in the treated plasmid (**Fig. 6**). In the electrophoregram, the untreated

plasmid DNA, used as control, has the major supercoiled Form I and minor singly nicked relaxed circular Form II bands. However, for **1b**, **1c**, **1e**, and **1f**, they showed Form II bands of linear DNA. These results show that the compounds cleave the DNA in both strands.

**Fig. 6 is here**

*3.2.8. Restriction enzyme digestion*

To gain further insight into the changes in DNA confirmation, the compounds-DNA incubation, as shown above, was followed by *Bam*H1 or *Hind*III digestion. **Fig. 7** shows the electrophoretograms applying to the interaction of plasmid DNA with one concentrations of each of the compounds.

**Fig.7 is here**

## 4. Conclusions

In conclusion, novel series of benzildihydrazone based Schiff bases **1a-h** have been prepared in good yields and successfully characterized by using FT-IR, $^{1}H/^{13}C$ NMR and HRMS. The structures of three of the prepared Schiff bases (**1d, 1e** and **1h**) have been verified by using single crystal X-ray diffraction methods. Again, the experimental results of the molecules were explained using DFT calculations. For applicability as optic dyes, TGA analyses were done for each dye. The compounds have been found to be stable and remained undecomposed at 300 $^{o}$C. This means that the compounds can be applicable as optic dyes. Compound **1f** has been noted to be potentially effective in suppressing microbial growth of bacteria with

variable potency towards *Bacillus subtilis* ATCC 6633, *Staphylococcus aureus* ATCC 25923, *Enterococcus faecalis* ATCC 29212. Also, **1f** has also been found to be a good potential for therapeutic uses against some Gram positive pathogens. It appears that, a compound with good antimicrobial activity against Gram-positive bacteria does not have any activity against Gram–negative bacteria. This may mean that, the activity is related to the differences in cell wall structure of the bacteria. In the case of compound-DNA interaction, all the compounds caused DNA fragmentation.

Finally, we believe that, the compounds will have potential application as chemsensors for any cation or can be precursor ligands for some metals. The investigation of their chemosensor properties and affinity towards some metal is currently ongoing and results found scientifically viable will be published sooner.

**Acknowledgements**

The authors are very grateful to Gazi University Research Fund for providing financial support for this project (grant No. 05/2009-43). The numerical calculations reported in this paper were fully performed at TUBITAK ULAKBIM, High Performance and Grid Computing Center (TRUBA resources).

**Appendix A. Supplementary data**

Supplementary data related to this article can be found at…….

**References**

[1] H. Schiff, The syntheses and characterization of Schiff base, Ann. Suppl., 1864, 3, 343.

[2] E. Keskioglu, A.B. Gunduzalp, S. Cete, F. Hamurcu, B. Erk, Cr (III), Fe (III) and Co (III) complexes of tetradentate (ONNO) Schiff base ligands: synthesis, characterization, properties and biological activity. Spectrochimica Acta Part A: Molecular and Biomolecular Spectroscopy 70.3 (2008): 634-640.

[3] Abu-Hussen, Azza A.A., Synthesis and spectroscopic studies on ternary bis-Schiff-base complexes having oxygen and/or nitrogen donors. Journal of Coordination Chemistry 59.2 (2006): 157-176.

[4] Singh, Kiran, Manjeet Singh Barwa, and Parikshit Tyagi, Synthesis, characterization and biological studies of Co (II), Ni (II), Cu (II) and Zn (II) complexes with bidentate Schiff bases derived by heterocyclic ketone. European Journal of Medicinal Chemistry 41.1 (2006): 147-153.

[5] P. Panneerselvam, R.R. Nair, G. Vijayalakshmi, E.H. Subramanian, S.K. Sridhar, Synthesis of Schiff bases of 4-(4-aminophenyl)-morpholine as potential antimicrobial agents. European journal of medicinal chemistry 40.2 (2005): 225-229.

[6] (a) Chohan, Zahid Hussain, and Samina KAUSAR, Synthesis, structural and biological studies of nickel (II), copper (II) and zinc (II) chelates with tridentate Schiff bases having NNO and NNS donor systems. Chemical and Pharmaceutical Bulletin 41.5 (1993): 951-953.;

(b) Thomson, Andrew J., and Harry B. Gray, Bio-inorganic chemistry. Current opinion in chemical biology 2.2 (1998): 155-158.

[7] L.H. Abdel-Rahman, A.M. Abu-Dief, R.M. El-Khatib, S.M. Abdel-Fatah, Some new nano-sized Fe (II), Cd (II) and Zn (II) Schiff base complexes as precursor for metal oxides:

Sonochemical synthesis, characterization, DNA interaction, in vitro antimicrobial and anticancer activities, Bioorganic chemistry, 69 (2016) 140-152.

[8] M. Abo-Aly, A. Salem, M. Sayed, A.A. Aziz, Spectroscopic and structural studies of the Schiff base 3-methoxy-N-salicylidene-o-amino phenol complexes with some transition metal ions and their antibacterial, antifungal activities, Spectrochimica Acta Part A: Molecular and Biomolecular Spectroscopy, 136 (2015) 993-1000.

[9] M. Shebl, Synthesis, spectroscopic characterization and antimicrobial activity of binuclear metal complexes of a new asymmetrical Schiff base ligand: DNA binding affinity of copper (II) complexes, Spectrochimica Acta Part A: Molecular and Biomolecular Spectroscopy, 117 (2014) 127-137.

[10] M.M. Abd-Elzaher, A.A. Labib, H.A. Mousa, S.A. Moustafa, M.M. Ali, A.A. El-Rashedy, Synthesis, anticancer activity and molecular docking study of Schiff base complexes containing thiazole moiety, Beni-Suef University Journal of Basic and Applied Sciences, 5 (2016) 85-96.

[11] J.-R. Duan, H.-B. Liu, P. Jeyakkumar, L. Gopala, S. Li, R.-X. Geng, C.-H. Zhou, Design, synthesis and biological evaluation of novel Schiff base-bridged tetrahydroprotoberberine triazoles as a new type of potential antimicrobial agents, MedChemComm, 8 (2017) 907-916.

[12] Y. Jia, J. Li, Molecular assembly of schiff base interactions: construction and application, Chemical reviews, 115 (2014) 1597-1621.

[13] S. Zehra, M. Shavez Khan, I. Ahmad, F. Arjmand, New tailored substituted benzothiazole Schiff base Cu (II)/Zn (II) antitumor drug entities: effect of substituents on DNA binding profile, antimicrobial and cytotoxic activity, Journal of Biomolecular Structure and Dynamics, (2018) 1-17.

[14] D. Sriram, P. Yogeeswari, N.S. Myneedu, V. Saraswat, Abacavir prodrugs: Microwave-assisted synthesis and their evaluation of anti-HIV activities, Bioorganic and medicinal chemistry letters, 16 (2006) 2127-2129.

[15] W.H. Mahmoud, R.G. Deghadi, G.G. Mohamed, Novel Schiff base ligand and its metal complexes with some transition elements. Synthesis, spectroscopic, thermal analysis, antimicrobial and in vitro anticancer activity, Applied Organometallic Chemistry, 30 (2016) 221-230.

[16] Bulaov A O, Lukyanov B S, Kogan V A, Lukov V V, Photo- and thermochromic spirans. New metal chelates based on azomethines and hydrazones containing a spiropyran fragment, Russ J. Coord. Chem. 28 (2002), 46-49, DOI 10.1023/A:1013715821212.

[17] Al-Assar F, Zelenin K N, Lesiovskaya E E, Bezhan I P, Chakchir B A, Synthesis and Pharmacological Activity of 1-Hydroxy-, 1-Amino-, and 1-Hydrazino-Substituted 2,3-Dihydro-1H-pyrazolo[1,2-a]pyridazine-5,8-diones and 2,3-Dihydro-1H-pyrazolo[1,2-b] phtha-lazine-5,10-diones, Pharm Chem J. 36 (2002), 598-603, DOI 10.1023/A:1022665331722.

[18] Sharma V K, Srivastava S, Synthesis, Spectroscopic and Antifungal Studies of Trivalent Chromium, Manganese, Iron and Cobalt Complexes with Hydrazones derived from Benzil –monoxime and various Aromatic Hydrazides, Synt. React. Inorg. Met. Org. Nano. Met. Chem. 35 (2005), 311-318, DOI10.1081/SIM-200055249.

[19] Murukan B, Mohanan K, Synthesis, Characterization, Electrochemical Properties and Antibacterial Activity of Some Transiton Metal Complexes with [(2-hydroxy-1-naphthaldehyde)-3-isatin]-bishydrazone, Transition Met. Chem. 31 (2006), 441-446, DOI 10.1007/s11243-006-0011-7.

[20] Edward E I, Epton R, Marr G, Organometallic derivatives of penicillins and cephalosporins a new class of semi-synthetic antibiotics, J. Organomet. Chem. 85 (1975), C23-C25, DOI 10.1016/S0022-328X(00)80708-1.

[21] Pandey J K, Pandey O P, Sengupta S K, Synthesis and spectroscopic investigations of oxovanadium (IV) derivatives with 1,1'-diacetylferrocenylbis( hydrazones), Indian J. Chem. 43A (2004), 1906-1910.

[22] Vatsa B G, Pandey O P, Sengupta S K, Synthesis, Spectroscopic andToxicity Studies of Titanocene Chelates of Isatin-3-Thiosemicarbazones, Bioinorg. Chem. Appl. 3 (2005), 151-160, DOI 10.1155/BCA.2005.151.

[23] Libin Zang, Shimei Jiang, Substituent effects on anion sensing of salicylidene Schiff base derivatives: Tuning sensitivity and selectivity. Spectrochimica Acta Part A: Molecular and Biomolecular Spectroscopy 150 (2015) 814–820.

[24] Issah Yahaya, Meryem Chemchem, Burcu Aydıner, Nurgül Seferoğlu, Fulya Erva Tepe, Leyla Açık, Nebahat Aytuna Çerçi, Mustafa Türk, Zeynel Seferoğlu, Novel Coumarin-Thiophene-Derived Schiff Bases: Synthesis, Effects of Substituents, Photophysical Properties, DFT Calculations, and Biological Activities. Journal of Photochemistry & Photobiology A: Chemistry 368 (2019) 296–306.

[25] J. R. Anacona, N. Noriega, J. Camus, Synthesis, characterization and antibacterial activity of a tridentate Schiff base derived from cephalothin and sulfadiazine, and its transition metal complexes. Spectrochimica Acta - Part A: Molecular and Biomolecular Spectroscopy. 137 (2015) 16–22.

[26] Bagihalli G. B., Avaji P. G., Patil S. A., Badami P. S., Synthesis, spectral characterization, in vitro antibacterial, antifungal and cytotoxic activities of Co(II), Ni(II) and Cu(II) complexes with 1,2,4-triazole Schiff bases. European Journal of Medicinal Chemistry. 2008;43(12):2639–2649.

[27] S. Amer, N. El-Wakiel, H. El-Ghamry, Synthesis, spectral, antitumor and antimicrobial studies on Cu(II) complexes of purine and triazole Schiff base derivatives. Journal of Molecular Structure, 1049 (2013) 326–335.

[28] B.-L. Fei, W.-S. Xu, W.-L. Gao, J. Zhang, Y. Zhao, J.-Y. Long, C.E. Anson, A.K. Powell, DNA binding and cytotoxicity activity of a chiral iron (III) triangle complex based on a natural rosin product, Journal of Photochemistry and Photobiology B: Biology, 142 (2015) 77-85.

[29] P. Gotwals, S. Cameron, D. Cipolletta, V. Cremasco, A. Crystal, B. Hewes, B. Mueller, S. Quaratino, C. Sabatos-Peyton, L. Petruzzelli, Prospects for combining targeted and conventional cancer therapy with immunotherapy, Nature Reviews Cancer, 17 (2017) 286.

[30] C.C. Wang, S.M. Wu, H.W. Li, H.T. Chang, Biomedical Applications of DNA-Conjugated Gold Nanoparticles, ChemBioChem, 17 (2016) 1052-1062.

[31] J. Shawon, A.M. Khan, A. Rahman, M.M. Hoque, M.A.K. Khan, M.G. Sarwar, M.A. Halim, Molecular recognition of azelaic acid and related molecules with DNA polymerase I investigated by molecular modeling calculations, Interdisciplinary Sciences: Computational Life Sciences, (2016) 1-13.

[32] H. Sun, J. Ren, X. Qu, Carbon nanomaterials and DNA: From molecular recognition to applications, Accounts of chemical research, 49 (2016) 461-470.

[33] G. Elmacı, E. Aktan, N. Seferoğlu, T. Hökelek, Z. Seferoğlu, Synthesis, molecular structure and computational study of (Z)-2-((E)-4-nitrobenzylidene) hydrazone)-1, 2-diphenylethan-1-one, Journal of Molecular Structure, 1099 (2015) 83-91.

[34] R. Chandra, A. Ghorai, G. K. Patra, A simple benzildihydrazone derived colorimetric and fluorescent ‘on–off-on’ sensor for sequential detection of copper(II) and cyanide ions in aqueous solution, Sensors and Actuators B 255 (2018) 701–711.

[35] D.L. Mayers, J.D. Sobel, M. Ouellette, K.S. Kaye, D. Marchaim, Antimicrobial Drug Resistance C: Clinical and Epidemiological Aspects, vol. 2, Springer Dordrecht Heidelberg, London (2009) 681–1347.

[36] C.C. Wang, S.M. Wu, H.W. Li, H.T. Chang, Biomedical Applications of DNA-Conjugated Gold Nanoparticles, ChemBioChem, 17 (2016) 1052-1062.

[37] J. Shawon, A.M. Khan, A. Rahman, M.M. Hoque, M.A.K. Khan, M.G. Sarwar, M.A. Halim, Molecular recognition of azelaic acid and related molecules with DNA polymerase I investigated by molecular modeling calculations, Interdisciplinary Sciences: Computational Life Sciences, (2016) 1-13.

[38] H. Sun, J. Ren, X. Qu, Carbon nanomaterials and DNA: From molecular recognition to applications, Accounts of chemical research, 49 (2016) 461-470.

[39] G. Elmacı, E. Aktan, N. Seferoğlu, T. Hökelek, Z. Seferoğlu, Synthesis, molecular structure and computational study of (Z)-2-((E)-4-nitrobenzylidene) hydrazone)-1, 2-diphenylethan-1-one, Journal of Molecular Structure, 1099 (2015) 83-91.

[40] G. Elmacı, H.Duyar, B.Aydıner, N. Seferoğlu, Mir A. Naziri, E. Şahin, Z. Seferoğlu, The syntheses, molecular structure analyses and DFT studies on new benzil monohydrazone based Schiff bases, Journal of Molecular Structure, 1162 (2018) 37-44.

[41] I. Rigaku/MSC, 9009 new Trails Drive, TheWoodlands, TX 77381, USA.

[43] G.M. Sheldrick, Program for crystal structure solution and refinement, SHELXS-97 and SHELXL-97, (1997).

[44] M. Frisch, G. Trucks, H.B. Schlegel, G. Scuseria, M. Robb, J. Cheeseman, G. Scalmani, V. Barone, B. Mennucci, G. Petersson, Gaussian 09, revision a. 02, gaussian, Inc., Wallingford, CT, 200 (2009).

[45] R. Bauernschmitt, R. Ahlrichs, Treatment of electronic excitations within the adiabatic approximation of time dependent density functional theory, Chemical Physics Letters, 256 (1996) 454-464.

[46] M. Cossi, V. Barone, Time-dependent density functional theory for molecules in liquid solutions, The Journal of chemical physics, 115 (2001) 4708-4717.

[47] M. Wieland, W. Seichter, A. Schwarzer, E. Weber, Influence of different aryl substitution on the crystal structures of benzil monohydrazone and dibenzil azine parent compounds, Structural Chemistry, 22 (2011) 1267.

[48] X.-H. Li, X.-R. Liu, X.-Z. Zhang, Molecular structure and vibrational spectra of three substituted 4-thioflavones by density functional theory and ab initio Hartree–Fock calculations, Spectrochimica Acta Part A: Molecular and Biomolecular Spectroscopy, 78 (2011) 528-536.

[49] T.L. Greaves, C.J. Drummond, Protic ionic liquids: properties and applications, Chemical reviews, 108 (2008) 206-237.

# CAPTIONS

**Scheme Captions;**

**Scheme 1.** The synthetic pathway of synthesis of benzildihydrazone derivatives.

**Figure Captions;**

**Fig. 1. (a)** Crystal structure of the compound **1d** with atom labeling scheme. Thermal ellipsoids are drawn at the 40% probability level. **(b)** Unit cell with the layered structure of the molecule in the crystal.

**Fig. 2.** Crystal structure of the compounds **1e (a)** and **1h (b)** with atom labeling scheme. Thermal ellipsoids are drawn at the 40% probability level.

**Fig. 3**. The optimized geometry of all studied molecules (**1a**-**1h**).

**Fig. 4**. Temperature dependence of thermodynamic quantities (C, S and ΔH) for **1d**, **1e** and **1h**.

**Fig. 5.** TGA-DTA thermograms of **1a-1h** samples.

**Fig. 6.** Electrophotograms applying to the interaction of plasmid DNA with decreasing concentrations of **1a**, **1b**, **1c,1d, 1e, 1f, 1g** and **1h**. Lane P applied untreated plasmid DNA to serve as a control. Lines 1-5 applied to plasmid DNA interacted with decreasing concentrations of compounds (4000 µM, 2000 µM, 1000 µM, 500 µM).

**Fig. 7.** Electrophoretogram applying to incubated mixtures of plasmid DNA and compounds **1a**, **1b**, **1c,1d, 1e, 1f, 1g** and **1h** followed by digestion with *Bam*H1 or *Hind*III. Lane P applied to the untreated and undigested plasmid DNA. Lane P/B or P/H applied to untreated, but digestion with restriction enzyme *Bam*H1 or *Hind*III, respectively. Results shows that all of the compounds inhibited enzyme digestion indicating compounds binding A/A and G/G nucleotides on DNA.

**Table Captions;**

**Table 1.** The calculated and experimental absorption maxima ($\lambda_{max}$) values and oscillator strength (*f*), transitions with the absolute CI coefficient values obtained in the calculations.

**Table 2.** Antimicrobial activity of the compound (4000µM) expressed as inhibition zones (mm) (amp= ampicillin, C= chloramphenicol and K= ketoconazole).

**Table 1.** The calculated and experimental absorption maxima ($\lambda_{max}$) values and oscillator strength (*f*), transitions with the absolute CI coefficient values obtained in the calculations.

| | | $\lambda_{max}^{exp.}$ (nm) | Absorbance | $\lambda_{max}^{cal.}$ (nm) | *f* | transitions | CI |
|---|---|---|---|---|---|---|---|
| **1a** | DMSO | 322 | 0.056 | 347 | 1.2964 | H-1→L+1 | 0.57295 |
| | | | | | | H→L | 0.40828 |
| | Chloroform | 309 | 0.444 | 347 | 1.3024 | H-1→L+1 | 0.57661 |
| | | | | | | H→L | 0.40218 |
| **1b** | DMSO | 343 | 0.071 | 419 | 0.8765 | H→L+1 | 0.61585 |
| | Chloroform | 331 | 0.338 | 415 | 0.9011 | H→L+1 | 0.61663 |
| **1c** | DMSO | 322 | 0.083 | 367 | 1.3445 | H-1→L+1 | 0.54285 |
| | | | | | | H→L | 0.38819 |
| | Chloroform | 317 | 0.419 | 368 | 1.3367 | H-1→L+1 | 0.48812 |
| | | | | | | H→L | 0.36699 |
| **1d** | DMSO | 327 | 0.053 | 354 | 1.4126 | H-1→L+1 | 0.59218 |
| | | | | | | H→L | 0.38095 |
| | Chloroform | 317 | 0.514 | 355 | 1.4175 | H-1→L+1 | 0.59536 |
| | | | | | | H→L | 0.37548 |
| **1e** | DMSO | 343 | 0.018 | 353 | 1.3942 | H-1→L | 0.39211 |
| | | | | | | H→L+1 | 0.58451 |
| | Chloroform | 313 | 0.364 | 353 | 1.3839 | H-1→L | 0.39742 |
| | | | | | | H→L+1 | 0.58058 |
| **1f** | DMSO | 340 | 0.089 | 362 | 1.2957 | H-1→L | 0.38292 |
| | | | | | | H→L+1 | 0.57546 |
| | Chloroform | 324 | 0.096 | 361 | 1.3276 | H-1→L | 0.35479 |
| | | | | | | H→L+1 | 0.55157 |
| **1g** | DMSO | 329 | 0.085 | 368 | 1.2432 | H→L | 0.21615 |
| | | | | | | H→L+1 | 0.55262 |
| | Chloroform | 327 | 0.524 | 367 | 1.3148 | H→L | 0.24791 |
| | | | | | | H→L+1 | 0.53218 |
| **1h** | DMSO | 397 | 0.073 | 423 | 1.1946 | H-1→L | 0.28995 |
| | | | | | | H→L+1 | 0.64184 |
| | Chloroform | 380 | 0.288 | 414 | 1.2098 | H-1→L | 0.27648 |
| | | | | | | H→L+1 | 0.64697 |

**Table 2.** Antimicrobial activity of the compound (4000µM) expressed as inhibition zones (mm) (amp= ampicillin, C= chloramphenicol and K= ketoconazole).

| | ***Bacillus subtilis*** **ATCC 6633** | ***Staphylococcus aureus*** **ATCC 25923** | ***Enterococcus faecalis*** **ATCC 29212** |
|---|---|---|---|
| **Amp** | 23 ± 1 | 44 ± 1 | 27 ± 0 |
| **C** | 21 ± 0 | 24 ± 1 | 20 ± 0 |
| **1f** | 15 ± 0 | 13,33 ± 0,577 | 14,67 ± 0,577 |

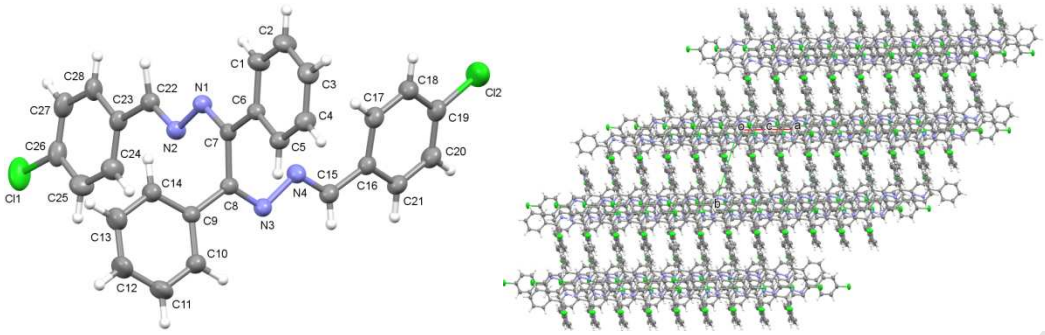


**(a)** **(b)**

**Fig. 1. (a)** Crystal structure of the compound **1d** with atom labeling scheme. Thermal ellipsoids are drawn at the 40% probability level. **(b)** Unit cell with the layered structure of the molecule in the crystal.

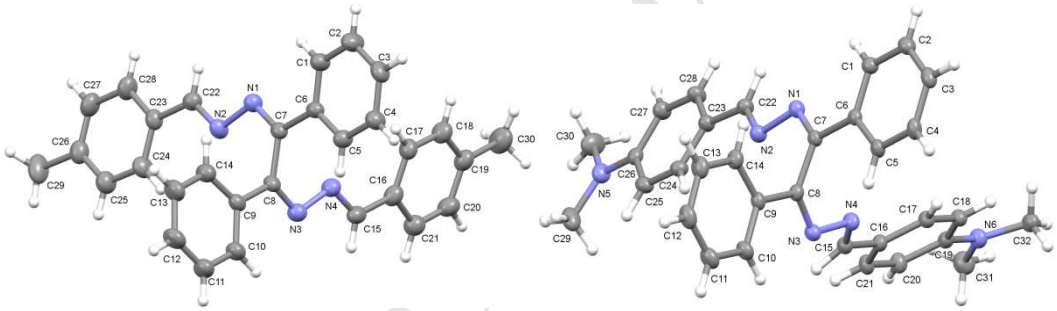


**(a)** **(b)**

**Fig. 2.** Crystal structure of the compounds **1e (a)** and **1h (b)** with atom labeling scheme. Thermal ellipsoids are drawn at the 40% probability level.

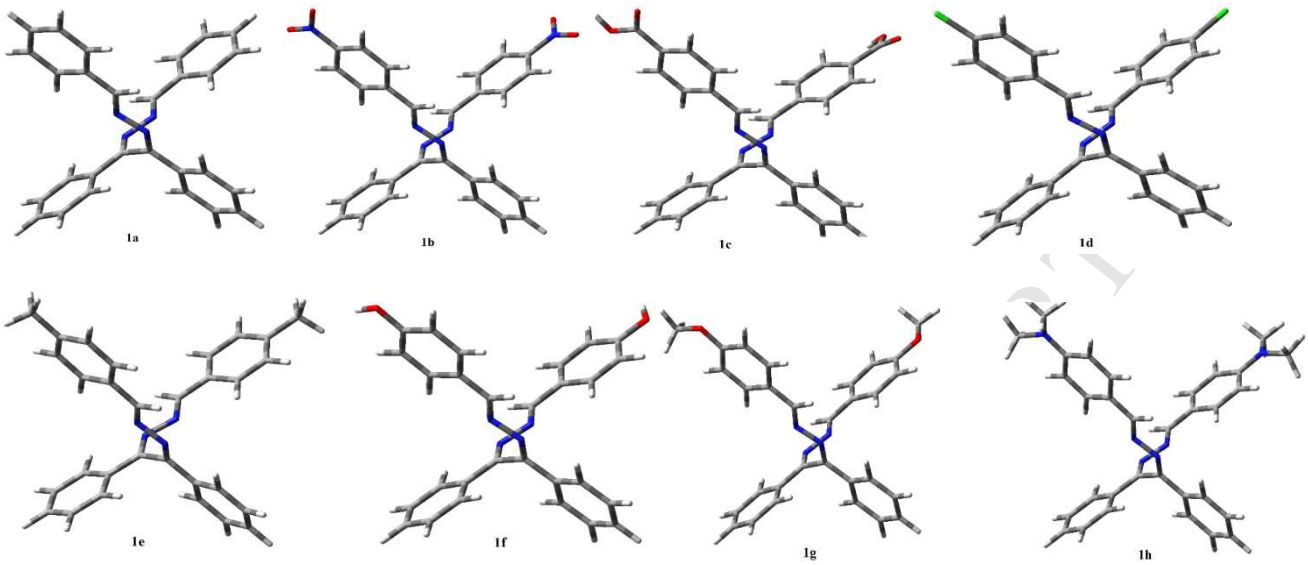


**Fig. 3**. The optimized geometry of all studied molecules (**1a**-**1h**).

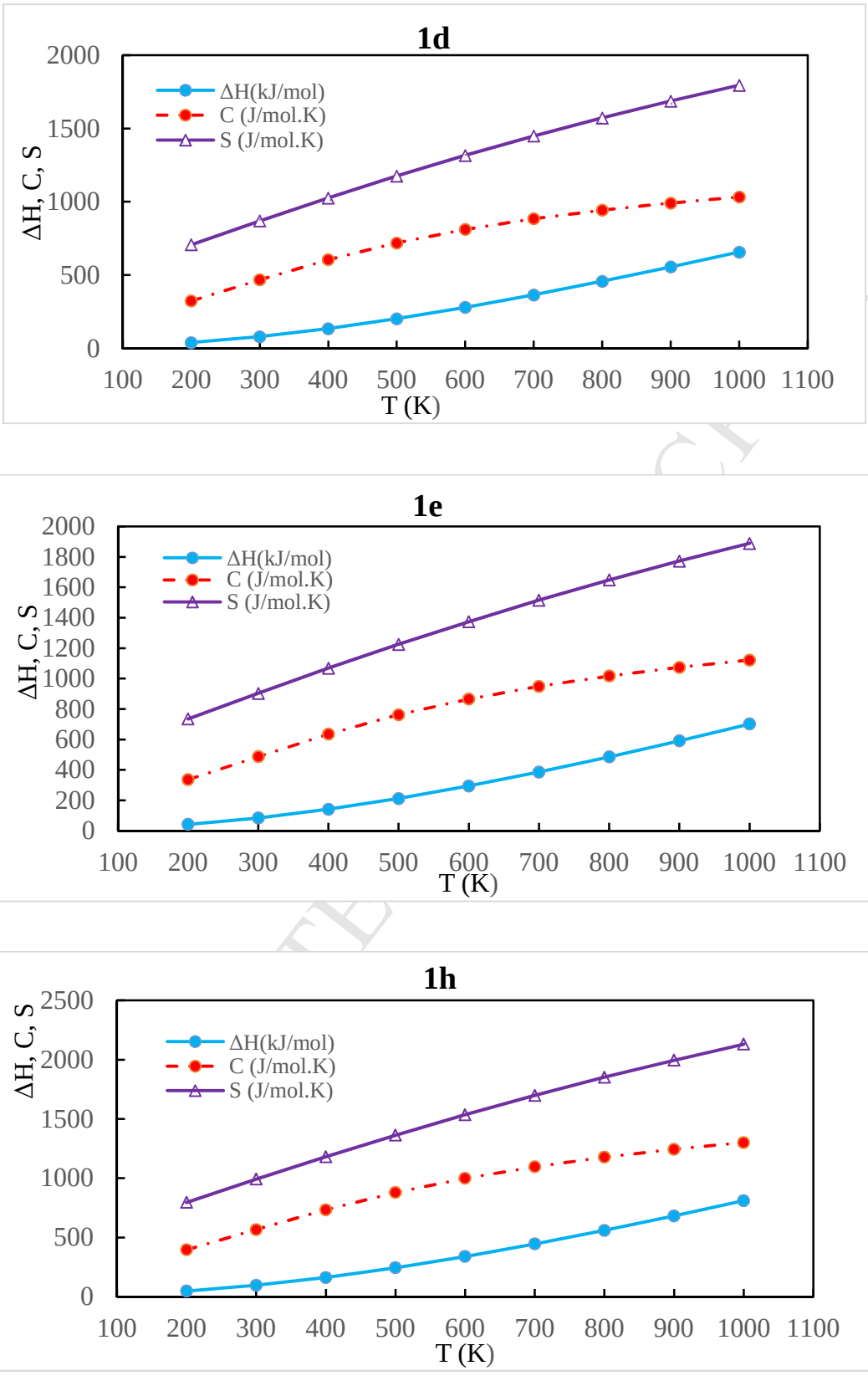


**Fig. 4**. Temperature dependence of thermodynamic quantities (C, S and ΔH) for **1d**, **1e** and **1h**.

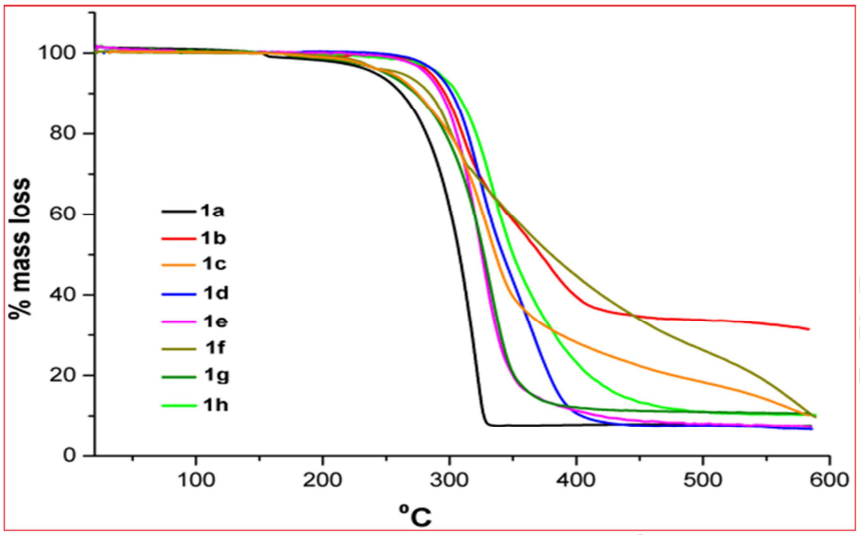


**Fig. 5.** TGA-DTA thermograms of **1a-1h** samples.

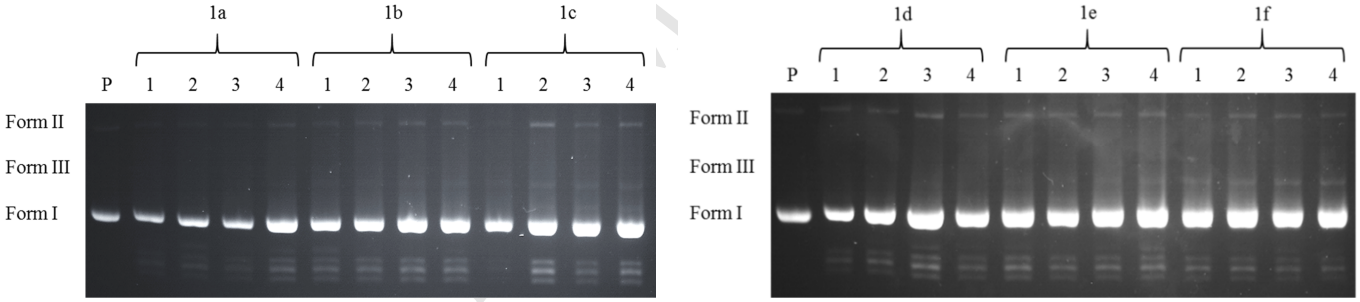


**Fig. 6.** Electrophotograms applying to the interaction of plasmid DNA with decreasing concentrations of **1a**, **1b**, **1c,1d, 1e, 1f, 1g** and **1h**. Lane P applied untreated plasmid DNA to serve as a control. Lines 1-5 applied to plasmid DNA interacted with decreasing concentrations of compounds (4000 µM, 2000 µM, 1000 µM, 500 µM).

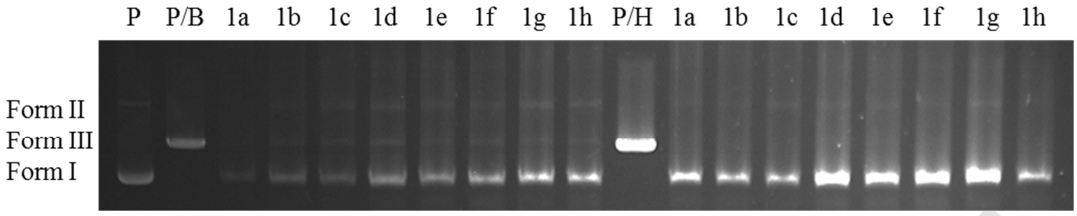


**Fig. 7.** Electrophoretogram applying to incubated mixtures of plasmid DNA and compounds **1a**, **1b**, **1c,1d, 1e, 1f, 1g** and **1h** followed by digestion with *Bam*H1 or *Hind*III. Lane P applied to the untreated and undigested plasmid DNA. Lane P/B or P/H applied to untreated, but digestion with restriction enzyme *Bam*H1 or *Hind*III, respectively. Results shows that all of the compounds inhibited enzyme digestion indicating compounds binding A/A and G/G nucleotides on DNA.

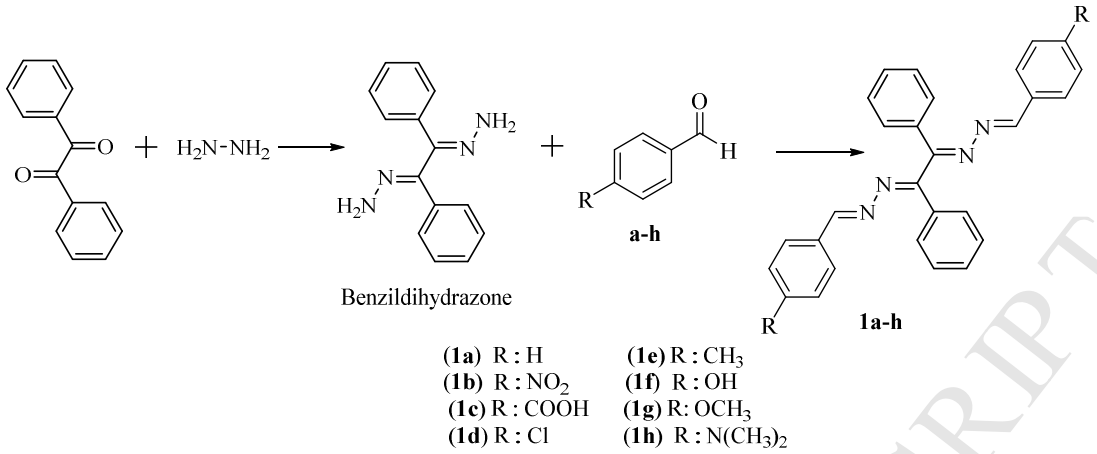


**Scheme 1.** The synthetic pathway for the benzildihydrazone based Schiff bases **1a-h**.

## Highlights

- A novel series of benzildihydrazone based Schiff bases were synthesized and characterized.
- The obtained experimental results were explained by DFT.
- The compounds were found to be stable at temperature beyond 300 $^{o}$C.
- Compound **1f** has been noted as potentially effective in suppressing microbial growth of some bacteria.
- All the prepared Schiff bases have found to recognize specific sequences and structures of nucleic acids for development of new therapeutics.